A broadband UAV-Based FMCW GPR and the Influence of Vegetation

Ralf Burr*, Markus Schartel†, Winfried Mayer‡, Thomas Walter*, and Christian Waldschmidt†
*Laboratory of Microtechnology, Ulm University of Applied Sciences, 89075 Ulm, Germany
†Institute of Microwave Engineering, Ulm University, 89081 Ulm, Germany
‡Endress+Hauser GmbH+Co. KG, 79689 Maulburg, Germany
Email: burr@hs-ulm.de

***Abstract*—Ground penetrating radar (GPR) is one of the tools supporting mine detection. In this contribution a wide-band frequency-modulated-continuous wave (FMCW) GPR operating in the frequency band from 0.6 GHz to 4.6 GHz in a bistatic configuration is presented. The frequency synthesis is realized using a broadband voltage controlled oscillator (VCO) in a higher frequency band and mixed down to the desired frequency band. The radar including antennas is integrated on a unmanned aerial vehicle (UAV). In measurements the effect of vegetation and the frequency dependence is investigated.**

***Index Terms*—ground penetrating radar, ultra wideband radar, unmanned aerial vehicles**

I. Introduction

Anti-personnel mines are weapons which are buried a few centimeters below the surface during wartime. They are designed to explode by the footstep of a person. After the end of the military conflict, these weapons remain in the ground and pose a permanent threat to the civilian population. In 2016, the Landmine Monitor recorded 8,605 casualties from these explosive remnants of war (ERW), of which at least 2,089 people were killed. According to UN estimates, approximately 60 to 70 million mines are still active in more than 70 countries [1].

GPR is a technology which has been used for more than 20 years to detect buried objects [2]. The currently used equipment for mine detection are mostly hand-held devices. The major disadvantage is that they have to be operated very close to the surface in potentially hazardous areas. To perform the GPR measurements from a safer distance, an approach is to mount the radar on a autonomous flying platform. Operating such a GPR in a side-looking orientation, the area throughput can be significantly increased in comparison to a downward looking arrangement. With regard to the restricted payload, a light-weight GPR was developed for operation on a UAV.

This paper is devided in five sections. After the introduction Section II presents the system concept and requirements for the GPR sensor. In Section III the sensor concept, the broadband frequency synthesis and the manufactured sensor is presented. The characterization of the sensor with a delay line as radar targets is presented in Section IV. Measurements with the GPR equipped UAV over vegetation is shown in Section V. Section VI gives a short conclusion.

II. System Concept and Requirements

For technical clearance, landmines must be detected down to a depth of 30 cm. Due to the fact that the attenuation increases with frequency, a frequency of up to 5 GHz is suitable for mine detection [3][4]. The lowest usable frequency is limited by the antenna size. With respect to the mechanical limitations, in particular weight and size, the frequency from 1 GHz to 4 GHz is selected. As shown in Fig. 1 the GPR sensor is mounted on a commercially available UAV. The 3D-printed horn antennas can be used in a frequency range from 0.6 GHz to 8.0 GHz and are presented in [5]. The radar measurements are stored on a single-board computer and evaluated offline after the flight.

Fig. 1: Carrier platform DJI M600 Pro equipped with two light-weight broadband antennas.

III. Sensor Concept and Realization

In the concept phase it was decided to use an FMCW radar. The main advantage of this modulation scheme is a higher mean energy that can be radiated compared to a pulse radar [2]. It also offers the possibility to filter out narrowband interference in the GPR frequency band. In a previous work, it was shown that it is advantageous to use a bistatic configuration and to seperate the receiver from the transmitter [6]. A schematic diagram of the radar module

ISBN 978-3-9812668-9-4

splitted into a main module which contains the transmitter and a secound module which contains the receiver is shown in Fig 2.

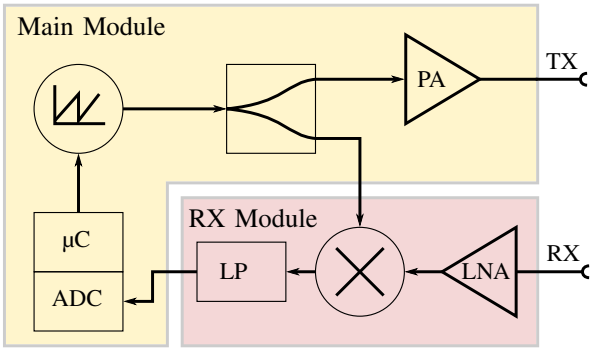

Fig. 2: Simplified block diagram of the distributed GPR sensor splitted into two modules.

A. Main Module

The stacked main module consists of the radio frequency (RF) frontend, power supply board, micro-controller board, as well as the communication interface board. The broadband frequency synthesization takes place on the RF frontend. The challenge of the synthesizer is to cover the frequency band of 3 GHz which corresponds to two frequency octaves. In order to realize this in an energy-saving way, a voltage-controlled oscillator (VCO) solution is used. Commercially available VCOs have a bandwidth of slightly more than one frequency octave. So it is not possible to cover the frequency band from 1 GHz to 4 GHz with a single VCO only. One option is to divide the frequency band into two sub-bands. Using a multiplier both frequency bands can be covered with one single VCO as shown in [6]. Its disadvantage is that the two frequency bands have to be merged after two measurements. As solution the frequency sweep is generated by an oscillator operating above the desired frequency band. A mixer is used to convert the frequency sweep down into the desired GPR frequency band. The schematic structure is shown in Fig. 3.

The core component of this structure is the diode mixer. It has an operating range from 6 GHz to 11 GHz and supports a bandwidth of more than 3 GHz. Due to its functional principle, it generates a harmonic of the RF as well as of the local oscillator (LO) input signal. These harmonics form further unwanted mixing products. If a LO frequency of 5 GHz is used, the 2nd harmonic frequency is 10 GHz. This harmonic of the LO is located directly in the operating range of the mixer and generates a mirrored mixing product in the operating range of the radar. To reduce this effect, the LO frequency is selected to be greater than the frequency of the broadband frequency sweep, e.g. 11 GHz. Now the harmonic is located far outside the operating regime of the mixer and is strongly attenuated. A simplified time frequency diagram is shown in Fig. 4.

Each VCO is stabilized with a fractional N phase locked loop (PLL). The PLL for the static frequency is running in the integer mode. For both PLLs a 1 GHz surface acoustic

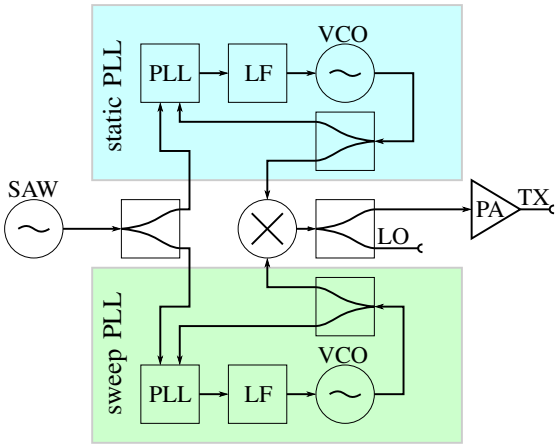

Fig. 3: Schematic structure of the frequency synthesis of the GPR frequency band using two PLLs.

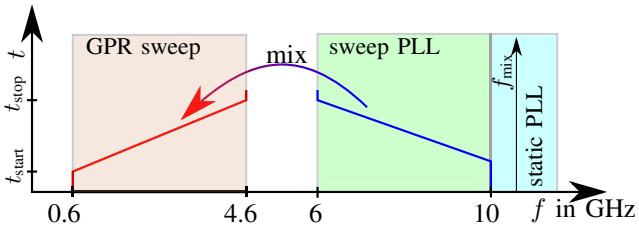

Fig. 4: Modulation domain diagram with the frequency range of sweep PLL and static PLL and the resulting GPR sweep.

wave (SAW) oscillator is used as reference. The phase detector frequency of both PLLs is 200 MHz. This prevents further mixing products being created by the interaction of the two PLLs. For a later expansion, the output of the sweep VCO is provided on an additional output port.

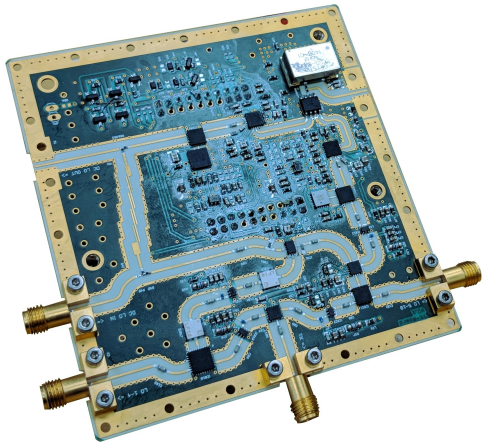

Fig. 5: RF frontend realized on a four-layer PCB.

Due to the internal structure of the VCO used for the static frequency generation, the spectrum of the output contains a spectral line with the half and the quarter frequency. These contributions are suppressed by 20 dB only. To further suppress these unwanted frequencies a parallel-coupled band-pass

ISBN 978-3-9812668-9-4

filter is used. The RF board consists of a hybrid layer structure of FR 4 and Rogers 4350 material. The assembled board is shown in Fig. 5.

B. RX Module

The RX module is a separate PCB, which can be directly mounted at the receiving antenna. The design is presented in the previous publication [6].

IV. Measurement Results

To check the function of the front end, a chirp at the LO port was recorded in the time domain and transformed into the frequency domain by means of short time Fourier transform. For this purpose the sweep PLL was programmed to performe a frequency sweep from 10 GHz to 6 GHz in 800 µs. The static PLL is operating at a frequency of 10.6 GHz. The result is shown in Fig. 6.

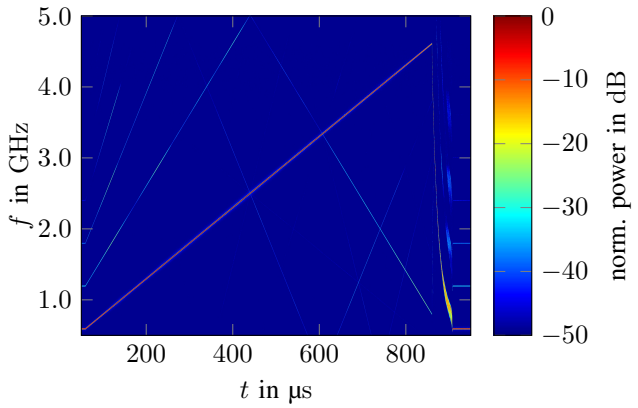

Fig. 6: Chirp from 0.6 GHz to 4.6 GHz recorded with an oscilloscope and transformed into frequency domain.

The result at the LO port is a frequency sweep from 0.6 GHz to 4.6 GHz. In the range up to 500 µs the harmonics of the frequency sweep can be identified. These are well suppressed by more than 30 dB. Starting from 700 µs to 850 µs a reverse passing spectral line to the sweep can be recognized. This is the down-converted harmonic of the sweep oscillator which reaches the operating range of the mixer. It is suppressed by more than 30 dB as well. The transmitting power at the TX port is 15 dBm.

In order to evaluate the overall system performance, the TX output port of the RF module is connected directly to the RX input port of the receiver board using a delay line. The signal path of the delay line corresponds to a target in 5 m distance. The total attenuation of the delay line with additional attenuators is 70 dB. For this measurements a frequency sweep from 1 GHz to 4 GHz in 1 ms is used. The recorded signal of a single radar measurement after the Fourier transform is shown in Fig. 7.

The target of the delay line is visible at 5 m. An insertable attenuation of 130 dB is achieved with this measurement. To evaluate the coherence of the radar 100 measurements are

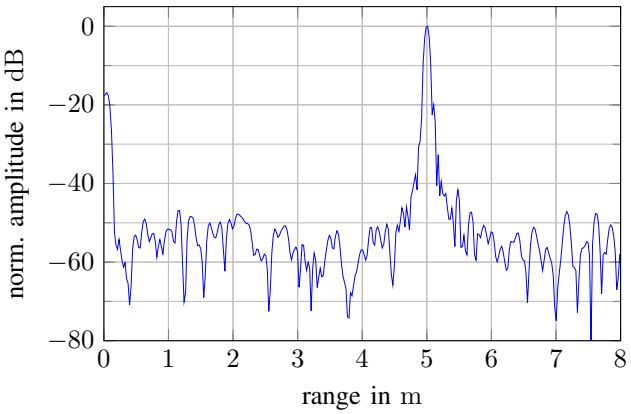

Fig. 7: Fourier transformed signal of the measurement using a delayline. The target range is 5 m.

performed and the phase of the target is extracted. The result is a maximum phase deviation of $\Delta\varphi_{\max} = \pm 2\,\mathrm{deg}$.

V. Measurement over Vegetation

Initial measurements are made over a dry corn field as shown in Fig. 8.

Fig. 8: Measurement field with two 30 dBsm corner reflectors and three −13 dBsm corner reflectors.

The measurement field is limited on the left and right side by a corner reflector. These are uncovered and lie at the edge between grain and meadow. Between these two reflectors there are three further reflectors with a radar cross section of −13 dBsm and a distance of approx. 1 m behind each other. The first reflector is on a line with the first two large reflectors and is not covered. The other two reflectors lie behind the first and are optically not visible due to the grain.

The flight path of the UAV is along the grain vegetated edge in a height of 2.5 m. During the flight, 406 measurements were recorded over a length of 15 m. The time domain data are transformed into the frequency domain and a synthetic aperture radar (SAR) image is focused with a back-projection algorithm [7].

ISBN 978-3-9812668-9-4

A. SAR Image

The processed SAR image with a bandwidth of 3 GHz is shown in Fig. 9.

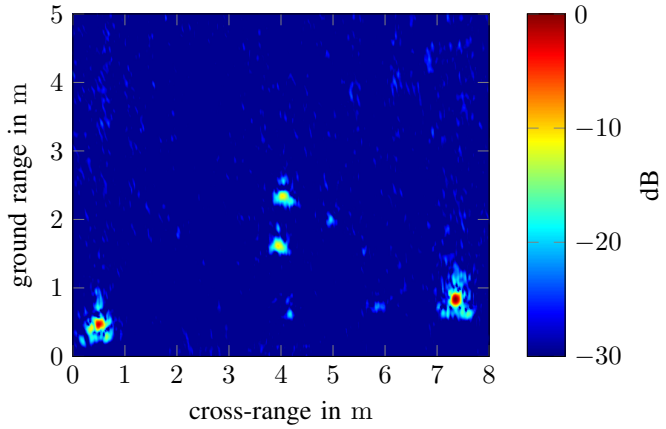

Fig. 9: SAR image of the setup shown in Fig 8.

In the processed image, only four of the five reflectors can be recognized unambiguously. The reflector in the middle, which is not covered, appears very weak. This is due to its faulty orientation.

B. Splitted Bandwidth

For further evaluation of the reflections, a cut is made through the right uncovered and the two covered reflectors along the ground range axis. The time domain data are divided into six sections, each corresponding to a sweep with 2 GHz bandwidth and a rising center frequency f_c from 2 GHz to 3 GHz. The result of the uncovered reflector is shown in Fig. 10 and that of the hidden reflector in Fig. 11. The SAR images with 2 GHz bandwidth are normalized with the same value as the SAR image with 3 GHz bandwidth.

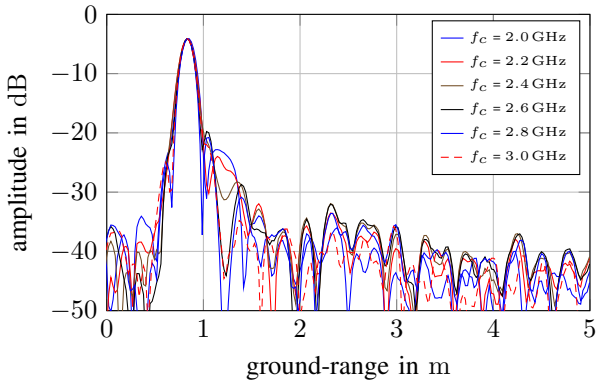

Fig. 10: Comparison of the amplitude of the uncovered reflector on the right side.

It can be seen that the amplitude of the reflection from the uncovered reflector is frequency independent. Comparing the amplitude with the covered reflectors it can be see, that the attenuation increases with the frequency. This means that dry

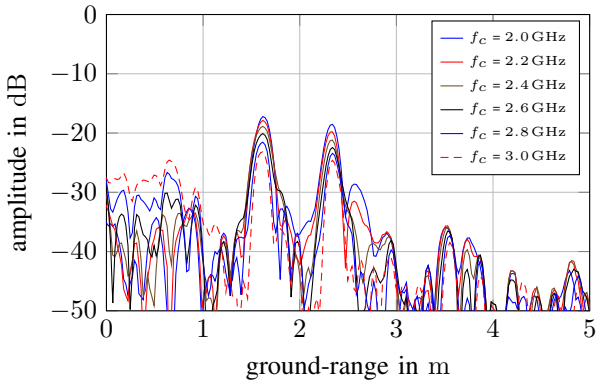

Fig. 11: Comparison of the amplitude of the two hidden reflectors in the middle of the test field.

grain with a residual moisture of approximately 15 volume percent leads to an attenuation of 5 dB when the center frequency is raised from 2 GHz to 3 GHz. This frequency dependence can be used for demining to classify between hidden and visible objects.

VI. Conclusion

A concept of a broadband FMCW GPR operating from 0.6 GHz to 4.6 GHz with a PLL-stabilized VCO frequency source was presented in this contribution. The function of the concept has been successfully evaluated by a synthesizer hardware design. The overall system performance was demonstrated by a cable measurement. Furthermore, the coherence of the entire system was successfully approved. The whole system was successfully integrated on a UAV and SAR image are taken over a grain field. By splitting the total bandwidth, the frequency-dependent attenuation by vegetation was shown.

Acknowledgment

The authors thank the Urs Endress foundation for supporting this work (https://www.ue-stiftung.org).

References

[1] The International Campaign to Ban Landmines, "Landmine monitor 2016," *Monitoring and Research Committee, ICBL-CMC Governance Board*, November 2016.

[2] D. Daniels, *Ground Penetrating Radar*, ser. Electromagnetics and Radar Series. Institution of Engineering and Technology, 2004, no. Bd. 1.

[3] C. Fischer and W. Wiesbeck, "Multistatic GPR for antipersonnel mine detection," in *IGARSS 2001*, vol. 6, 2001, pp. 2721–2723 vol.6.

[4] M. Fritzsche, *Anwendungen von Verfahren der Mustererkennung zur Detektion von Landminen mit Georadaren*. Universitt Karlsruhe, 2001.

[5] R. Burr, M. Schartel, W. Mayer, T. Walter, and C. Waldschmidt, "Lightweight broadband antennas for UAV based GPR sensors," in *48th European Microwave Conference (EuMC)*, September 2018, pp. 1–4.

[6] R. Burr, M. Schartel, P. Schmidt, W. Mayer, T. Walter, and C. Waldschmidt, "Design and implementation of a FMCW GPR for UAV-based mine detection," in *IEEE MTT-S International Conference on Microwaves for Intelligent Mobility (ICMIM 2018)*.

[7] M. Schartel, R. Burr, W. Mayer, N. Docci, and C. Waldschmidt, "UAV-based ground penetrating synthetic aperture radar," in *IEEE MTT-S International Conference on Microwaves for Intelligent Mobility (ICMIM)*, April 2018, pp. 1–4.